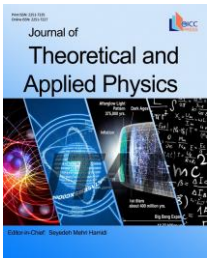

Volume 19, Issue 6, 192562 (1-11)

Journal of Theoretical and Applied Physics (JTAP)

https://doi.org/10.57647/j.jtap.2025.1906.62

Radiative Effect in MHD Flow of Viscoelastic Fluids with Null Mass Flux Through a Porous Channel

E. Esekhaigbe[1*], Uchenna A. Uka[2], Celestine. U Agwi[1] and A.B. Okrinya[3]

[1]*Department of Mathematics and Computer Science, University of Africa, Bayelsa State, Nigeria*

[2]*Department of Basic Sciences, School of Science and Technology, Babcock University, Ogun State, Nigeria*

[3]*Department of Mathematics, Niger Delta University, Bayelsa State, Nigeria*

***Corresponding author:** esekhaigbe.edwin@uat.edu.ng, steadystatesolution@gmail.com

Original Research

Received:
17 July 2025

Revised:
25 July 2025

Accepted:
17 October 2025

Publish online:
31 December 2025

Abstract

This study examined a viscoelastic fluid with zero mass flux, incorporating magnetohydrodynamics, radiative effects, melting heat effects, and channel permeability. The study of viscoelastic fluid is essential due to its extensive industrial and biological applications. The problem presented in the form of partial differential equations was converted into ordinary differential equations by a suitable similarity transformation. To solve the linked set of equations numerically, the Runge-Kuttab-Fehlberg fifth-order via shooting techniques, and Maple program were deployed. The resulting solution offers valuable insight into how melting heat and viscoelasticity interact to affect different flow characteristics. According to the profiles, the fluid's speed decreases due to an increase in the magnetic field and radiation parameters, but the velocity profile noticeably increases when the melting heat effect increases, showing an upward tendency in the fluid's speed. The temperature profile depicts a downward trend as the melting heat increases. The result indicates a low temperature distribution all through the fluid system. The study highlights how combining MHD, melting heat, and thermal effects is essential for the best performance and efficiency of viscoelastic fluids in cooling devices, oil recovery, polymer processing, and biomedical engineering.

Keywords: Melting heat; heat flux; MHD; Shrinking; MAPLE software

1. Introduction

Viscoelastic fluids are a class of complex fluids equipped with both viscous and elastic properties. Interestingly, such a fluid model represents a class of non-Newtonian fluids, providing opportunities to investigate the flow traits of materials that have viscoelastic properties. Understanding how Maxwell fluids interact with outside forces like magnetic fields, melting heat at solid boundaries, flow in porous media, and radiative effects is very intriguing to scientists and has real-world applications. In the study of viscoelastic fluids, magnetohydrodynamics (MHD) plays a crucial part. The interaction of magnetic fields with their viscoelastic properties can lead to some gripping or enthralling developments. The interaction between MHD and viscoelastic fluids has diverse uses in Biomedical engineering, cooling systems, food, and oil recovery, and polymer processing because of its turbulence drag reduction [1],[2] looked into MHD steady laminar flow and the radiative effects of heat moving from a laminar liquid to a melting surface that was moving. Thermal radiation and magnetic fields were included in their investigation, but fluid permeability was not [3] studied energy transfer and boundary layer flow in Maxwell fluids [4] looked at how heat moves through a vertical porous sheet that is always stretching. The fluids were Maxwell hybrid nanofluids.

The fluid's thermal transition was monitored using the hybrid nanofluid [5] studied the flow of a viscoelastic fluid through a stiff porous material [6] examined the Maxwell fluid's viscosity, relaxation duration, and

pressure effects. Since some viscoelastic fluids' material moduli depend on pressure, the solid component of their work was essential.

The study by [7] looked at the steady-state MHD flow in a flat, horizontal, permeable plate that had a Maxwell viscoelastic fluid in it, [8] examined the boundary layer flow and heat transport of a second-grade fluid at a stagnation point.

They combined melting heat transfer with Dufour and Sorex phenomena. They employed the series solution method to analyses their problem [9] used the Cattaneo-Christov model, the upper convective Maxwell fluid, and generalized fluid flow and heat flux on a porous, stretchy sheet. They use Legendre Collocation method in their investigation, [10] examined boundary layer flow in an upper-convicted Maxwell (UCM) fluid over a stretching sheet. [11] used a micro polar fluid to study stagnation point flow toward a horizontal linearly stretching or contracting sheet. They developed a model to investigate the heat transmission characteristics that take place during the melting process brought on by the stretching/shrinking sheet. Furthermore, looking at melting heat at the points where two solids meet adds a new level of complexity to viscoelastic fluid dynamics research. In industrial processes, melting or solidification at interfaces is a popular phenomenon. In heat transfer operations, it is vital to comprehend the action of solidification and its effects on the flow kinetics of viscoelastic fluids. These operations include chilling and steaming systems, solidification techniques in material science, and thermal management in electronic devices, among others. Understanding magnetohydrodynamics (MHD) and how melting affects solid boundaries at high temperatures is important for technological progress and makes it easier for people from different fields to study together. Our present endeavor seeks to investigate the interaction of these scenarios, uncovering insights that may catalyze innovation across several domains, such as aerospace, energy, engineering, and geophysical applications. This work aims to improve our understanding of fluid dynamics and its useful applications by making it clearer how viscoelastic fluids interact and behave when heated and magnetized fields are present at solid-liquid interfaces. The geometric modelling of MHD in a micropolar fluid by [12] looked at how radiation, melting energy, and viscous dissipation changed over an exponentially stretched sheet [13] looked into the different ways that energy moves through an entropy-optimized magnetic nanofluid. They incorporated melting energy transfer, joule heating, and a robust model in their study. The research by [14] looked at how mass and heat move through a sheet of Sisko nanofluid that is stretching in a way that is not linear. They took into account a heat source, MHD, and radiation [15] did an experiment to look into how phase-change heat transfer works in a horizontal cavity containing octadecane.

They added non-graphene and an electric field both passively and actively [16] looked at how a viscoelastic fractional-type Maxwell fluid naturally convicts as it flows over an inclined plate that moves back and forth. They employed the thickness vector thermal flux and generalized stress-shear equations. The research by [17] looked at how the flow, heat, and mass of a Maxwell fluid behaved over a stretching sheet that was inserted into a porous medium that let viscous heat escape. They used the spectrum relaxation method to examine the equations quantitatively [18] did a study on the Maxwell nanofluid that combined MHD and convection. They were interested in how heat moves when thermal radiation is present.

Their research elucidated the intricate relationships between chemical processes and fluid dynamics, providing insights into practical uses [19] examined the impact of wall slip conditions on temperature and the influence of Newtonian effects on heating. The study demonstrated the generalized memory effect using fractional Prabhakar derivatives. The research offers compelling insights into the influence of thermal factors on the behavior of Maxwell fluids in natural convection scenarios. A collection of works on Maxwell fluids in different geometries and parameter considerations can be found in [20]–[23].

Moreso, in the absence of variable thermal characteristics, the flow of Williamson fluid past the Riga plate was described by [24]. They discovered intriguing results using the shooting method, which show a decrease in the velocity distribution in the stretching ratio constant and viscosity parameter. In their investigation, they also noted that the existence of Boit numbers causes an increase in the movement of heat and energy.

In reference to lubricated surfaces, the flow of Williamson fluid on a power law has been described in [25]. The concentration and temperature equations are studied in conjunction with microorganisms, activation energy, Cattaneo-Christov mass, and heat flow. They used the MATLAB BVP4C solver, a powerful numerical tool for solving a system of coupled differential equations numerically. The passage of gyrotactic microorganisms via a porous tube in a non-Newtonian Casson-Williamson fluid was described in [26].

Their work is unusual since they use ion slip and Hall current. According to their research, the momentum boundary layer decreases for both Casson and Williamson parameters. Additionally, [27] investigated a constant flow of electro-magnetic hydrodynamics on a porous Casson-Williamson nanofluid cone that is exponentially vertical. They used the shooting method to implement the Runge-Kuttab-Fehlberg procedures [28] examined an unstable, three-dimensional rotating flow of non-Newtonian nanofluid as part of a chemical process fueled by activation energy across a porous region. The Casson-Williamson nanofluid has a higher viscosity than other fluids, which lowers the flow rate, according to their findings. Heat transmission under various conditions has been thoroughly studied and is available in [24], [29]–[33].

In a further advancement [34], disturbed Fourier's laws were taken into consideration when examining the magnetized flow of an Oldroyd-B fluid across a rotating disc by using the finite element approach. The thermal distribution on Oldroyd-B fluid was found to have a

decreasing trend in acceleration over the range of heat flux and thermal relaxation parameters.

The value of heat transmission decreases as the heat generating parameter increases.

Furthermore, when the strength of the homogeneous reaction grows, the fluid's absorption rate falls. The analysis of steady mixed convection flow close to a three dimensional non uniform vertical surface with slip effects was undertaken by [35]. In their analysis, a hybrid nano particle was used. Their findings showcased a higher heat transfer rate with the hybrid nano particle unlike the normal nanofluids.

Also, it was observed that mixed convection enhances the velocities of both hybrid and nano particle fluids while porosity diminishes their velocities. Similar work on hybrid nanofluids was carried out by [36], but theirs was MHD hybrid nanofluids with variable viscosities and thermal radiations.

The influence of thermal radiation and heat sink and source were performed and the results were similar to those obtained by [35].

A case of Fractional unsteady flow of viscoelastic hybrid nano fluids, fractional Maxwell viscoelastic nanofluid and their hybrid over a vertical channel are detailed in [37],[38].

More recent studies, including using artificial neural network into heat and mass transfer dynamics documented in [39]–[42].

This paper is structured as follows: The next subsection provides the literature gap and novelty. This portion is immediately followed by section two, titled 'Material and Methods' This section describes the mathematical formulation of the problem, the coordinate system and the flow direction. Furthermore, it provides details of the flow equations and captures the solution procedures adopted in this study.

The last section discusses the results and the implications of different parameters for velocity and temperature distributions. The key findings of this work are itemized in the concluding section.

In summary, the study's gap and research questions are itemizes below:

- This study considered heating effect with zero mass flux at boundaries with the inclusion of thermal radiation, MHD, and other parameters within a porous channel.
- How does magnetic field and thermal radiation affect fluid velocity?
- How imparted is fluid's velocity over a steady increase in the melting heat parameter?
- What is the effect of increasing Prandtl number parameter on fluid's temperature?

1.1 Literature Gap

The existing research has undoubtedly broadened our comprehension of the flow kinematics of vis- elastic fluids across various aspects, including chemical reactions, heat and mass transfer effects, and the addition of nanoparticles. The writers have effectively communicated their points and provided clear directions for various practical applications.

The referenced scholars executed their study by considering diverse fluids, geometries, and parameters. Nonetheless, the simultaneous melting heat effect and a null mass flux at the boundary, coupled with the radiative effect within a porous

channel, is a concept that was overlooked in their studies. So, this study puts these factors into context by looking at Maxwell fluid dynamics on a stretching sheet with melting heat effects and no mass flux.

The intricate interplay of diverse physical processes, the extensive array of practical applications, and the environmental implications render this a significant addition to the corpus of knowledge. A mathematical model governs the Maxwell fluid, utilizing the momentum and energy equations while incorporating magnetohydrodynamics and other intriguing parameters. We converted the $PDEs$ to $ODEs$ using the appropriate similarity transformations. We further deployed the $MAPLE$ software to quantitatively analyze the equations. The results of this study clarify how viscoelastic properties and melting heat effects affect various flow properties, such as temperature and velocity profiles. We expect the present work to be compelling and significantly advance the field of fluid dynamics. A few of the study's applications include:

- Polymer and food processing: Fluid movement or transport is core in majority of food processing industries. Viscous fluids are used in industries to make useful food products in bulk. Flow properties are the key basis of the mass transfer taking place in food industries.
- Material engineering: The model has broadened the understanding of viscoelastic fluids and their complex interaction with melting boundaries, This is very vital for process optimization and product quality.
- Shaping processes: Polymeric materials are usually performed in the liquid state over times that are rapid relative to those associated with molecule re-organization. This study, through viscoelasticity helps in understanding the flow and structure development of material shaping.

2. Material and Methods

The flow is steady and structured in the Cartesian coordinate system with the x-axis parallel to the surface and the y-axis normal to the surface. The flow is modelled along the type described in [8],[11]. Theirs focused on an unsteady flow of the boundary layer and energy transfer of a Maxwell fluid moving towards a flat sheet that is continuously melting with a warm liquid of the same type, while the present work focuses on steady flow as shown in Fig. 1. The sheet's velocity $u = U_w = a_x$ has been considered in the configuration where a is a positive constant associated with a stretching sheet. The free-stream temperature T_∞ and the temperature of the sheet T_m have both been considered and ($T_\infty > T_m$). We further assumed that the fluid maintains low electrical

conductivity, even when positioned above the sheet. The fluid is subject to a uniform transverse MHD whose intensity is denoted by T_m. We represent the fluid concentration, free-stream concentration, and sheet concentration as C, C_∞ and C_w respectively. The continuity, momentum, energy, and concentration equations are described in (1), (2), (3), and (4) respectively. The dimensionless (10), (11), and (12) are linked, non-linear, and admit no close form solution. The study combines the computational power of Runge Kuttab Fehlberg ($RKT45$) techniques and the shooting method to scrutinize the system numerically for different parameter values of interest. Pertinent profiles were provided using MAPLE software and the results are discussed qualitatively.

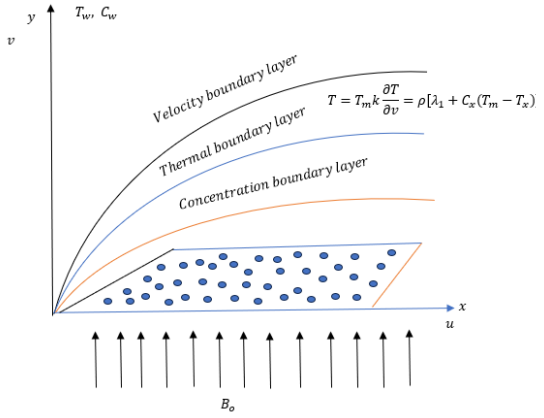

Figure 1. Physical model of the problem

The flow equations are stated below [8],[11].
Continuity equation:

$$\frac{\partial u}{\partial x} + \frac{\partial v}{\partial y} = 0 \tag{1}$$

Momentum equation:

The momentum equation emphasizes the fluid's motion.

It offers insights into the variations in fluid velocity and distribution upon contact with the stretched sheet.

$$\frac{\partial u}{\partial x} + v\frac{\partial u}{\partial y} + \lambda\left[u^2\frac{\partial^2 u}{\partial x^2} + v^2\frac{\partial^2 u}{\partial y^2} + 2uv\frac{\partial}{\partial x}\left(\frac{\partial u}{\partial y}\right)\right] = \mu\frac{\partial^2 u}{\partial y^2} - \frac{\sigma B_0^2}{\rho}\left[\lambda v\frac{\partial u}{\partial y} + u\right] - \frac{v}{k}u \tag{2}$$

Here, λ = relaxation time, ρ = fluid density, μ = kinematic viscosity, σ = electrical conductivity, and B_0 = magnetic field.

Energy equation:

The energy equation elucidates the allotment and transport of energy inside the fluid. It further delineates the conduct of viscoelastic fluids exhibiting distinct viscoelastic traits.

It encompasses terminology related to heat conduction, convection, heat generation and absorption, as well as any additional source or sink. In the absence of such factors, the objective would be to ascertain the overall behavior and principles that control heat transport in viscoelastic fluids.

$$u\frac{\partial T}{\partial x} + v\frac{\partial T}{\partial y} = \frac{\kappa}{\rho C_P}\frac{\partial^2 T}{\partial y^2} - \frac{1}{\rho C_P}\frac{\partial q_r}{\partial y} \tag{3}$$

From (3), u and v depict the elements due to x and y directions. Other fluid characteristics are specified as follows: ρ represents the fluid's density, σ denotes electrical conductivity, and C_p signifies the heat capacity at a fixed pressure, σ_s denotes the Stefan-Boltzmann constant, k^* represents absorption coefficient, and q_r signifies radiation.

In the context of viscoelastic fluid flow, the energy equation mathematically represents the balance of energy inside the fluid. It delineates the processes of heat generation, transportation, and dissipation while the fluid moves and engages its environment.

The equation took into account the viscoelastic characteristics of Maxwell fluids, which are elastic and viscous.

Further, using Ross land approximation [24], we have:

2.1. Microscopic single-particle shell model

$$q_r = \frac{-4\sigma^*\partial T^4}{3k^*\partial y} \tag{4}$$

Through Taylor series, T^4 is expanded about T_∞ , and the linear part is considered as:

$$T^4 = 4T_\infty^3 T - 3T_\infty^4 \tag{5}$$

By using Eqs. (4) and (5) in (3), we have:

$$u\frac{\partial T}{\partial x} + v\frac{\partial T}{\partial y} = \frac{\kappa}{\rho C_P}\frac{\partial^2 T}{\partial y^2} + \frac{16\sigma^* T_\infty^3}{3\rho C_P k^*}\frac{\partial^2 T}{\partial y^2} \tag{6}$$

Specie equation:

The specie or mass equation is an essential concept in fluid dynamics. It exemplifies the mathematical theory of conservation of mass. For a stretching sheet, it indicates that the fluid's density is fixed as it flows over the sheet, hence ensuring mass conservation within the system

$$u\frac{\partial C}{\partial x} + v\frac{\partial C}{\partial y} = D_B\frac{\partial^2 C}{\partial y^2} \tag{7}$$

Note that D_B represent mass diffusion, C is the fluid's concentration.

The dimensional BCs [43] are:

$$u = U_w = ax \ at \ y = 0,$$

$$u \to 0 \ at \ y = \infty, T = T_m \ at \ y = 0$$

$$k\frac{\partial T}{\partial y} = \rho[\lambda_1 + C_s(T_m - T_s)]v, at\ y = \infty$$
$$= and\ T = T_\infty \quad (8)$$
$$C = 0\ at\ y = 0, C \to C_\infty\ as\ y \to \infty$$

As described in Eq. (8), the sheet's velocity takes up the wall velocity denoted as U_w as y tends to infinity. The same behaviour applies to the temperature boundary condition, but at y = 0. Also, for the change in temperature with respect to the y-coordinate, the linear relationship between the viscoelastic fluid and density is represented as both y and T approaches infinity. For the species equation, the initial concentration is zero at y = 0 while both C and y tend to infinity. At this point we define zero mass flux boundary conditions as one in which the total mass transfer across a boundary is restricted. This indicates a disequilibrium between the mass entering the boundary and that exiting it. This leads to no net mass transfer. The transformational variables are explicitly defined in [44].

$$\mathrm{v} = -\sqrt{\mathrm{avh}(\eta)}, \mathrm{u} = \mathrm{axh}'(\eta), \eta = \left(\frac{\mathrm{a}}{\mathrm{v}}\right)^{\frac{1}{2}}\mathrm{y},$$
$$\psi = -\sqrt{(\mathrm{av})}\mathrm{xh}(\eta), \beta = \lambda\mathrm{a}, \mathrm{M} = \frac{\sigma \mathrm{B}_0^2}{\mathrm{a}\rho} \quad (9)$$
$$\theta = \frac{\mathrm{T} - \mathrm{T_m}}{\mathrm{T}_\infty - \mathrm{T_m}}, \mathrm{v} = -\sqrt{(\mathrm{av})}\mathrm{f}(\eta)$$
$$\mathrm{u} = \mathrm{axh}'(\eta), \mathrm{P_r} = \frac{\mathrm{v}}{\mathrm{a}}, \mathrm{S_c} = \frac{\mathrm{v}}{\mathrm{D_B}}, \phi = \frac{\mathrm{C}-\mathrm{C}_\infty}{\mathrm{C_w}-\mathrm{C}_\infty}$$

through the transformational variables, Eq. (9), Eqs. (2, 3 and 4) take the below forms:

$$\beta[2\mathrm{hh}'\mathrm{h}'' - \mathrm{h}^2\mathrm{h}'''] + \mathrm{h}''' + (\mathrm{h} + \mathrm{Mh})\mathrm{h}''$$
$$-\mathrm{h}'^2 - \mathrm{Kh}' = 0 \quad (10)$$

where $\beta = Deborah\ number$, M= Magnetic field, and K= Porosity

$$\frac{1}{P_r}(1 + R)\theta'' + h\theta' = 0 \quad (11)$$

Here, R and P_r represent radiation and Prandtl parameters.

$$\phi'' - \mathrm{S_c h}\phi' = 0 \quad (12)$$

Subject to the dimensionless BCs:

$$h'(0) = 1\ , \text{at}\ y = 0, h' = 0, \text{as}\ y = \infty$$
$$\theta(0) = 0, P_r h(0) + M_e\theta'(0) = 0 \quad (13)$$
$$\theta = 1\ \text{as}\ y = \infty$$
$$\phi = 0\ \text{at y= 0}, \phi' \to \infty\ \text{as}\ y = \infty$$

where M_e = melting heat effect parameter.

2.2. Verification of the Solution Technique

The approach is validated using a reference solution, as outlined by Uka et al. [45]. The Eqs. (10), (11), and (12), were solved using a fourth-order Runge–Kuttab–Fehlberg integration technique.

The suitable values for the unknown initial slopes $f(0)$ and $\theta(0)$ are determined through a shooting method. Here, we compare the calculated values of $f(\eta)$ and $\theta(\eta)$ as η approaches infinity [denoted as $\eta max(\to \infty) = 6$ with the prescribed boundary conditions $f(\infty) = 0$ and $\theta(\infty) = 0$.

The anticipated values of $f''(0)$ and $\theta'(0)$ are adjusted to obtain a refined approximation of the solution. The slopes $f''(0)$ and $\theta'(0)$ are iteratively estimated using Newton's method to ensure the boundary conditions are satisfied at the largest numerical values of $\eta \to \infty$.

Details on Choice of η∞, Initial Guesses, Tolerances, and Convergence Checks

1. Choice of η_∞:

- Definition: η∞ represents the numerical approximation of infinity in the context of boundary value problems, where the solution is expected to approach asymptotic behavior $(e.g., f(\infty) = 0\ and\ \theta(\infty) = 0)$.
- Value: The text specifies $\eta\max = 6$ as the practical choice for η∞. This value is chosen to ensure that the solution has sufficiently approached its asymptotic behavior within the computational domain.
- Rationale: The choice of $\eta_\infty = 6$ is based on prior numerical experiments or analytical insights, suggesting that beyond this point, the solution values ($f(\eta)$ and $\theta(\eta)$) stabilize and closely approximate their boundary conditions (0 in this case). The exact value depends on the problem's physical characteristics, such as the decay rate of the solution. A larger η∞ may increase computational cost without significant improvement, while a smaller value risks inaccurate results if the solution has not yet converged to its asymptotic state.
- Verification: The suitability of $\eta_\infty = 6$ is typically validated by testing larger values $(e.g., \eta = 7\ or\ 8)$ and confirming that the solution does not change significantly, ensuring the boundary conditions are met within the desired tolerance.

2. Initial Guesses:

- Context: The shooting method requires initial guesses for the unknown slopes $f''(0)$ and $\theta'(0)$ to solve the system of ordinary differential equations (ODEs) given by (10), (11), and (12).
- Selection: Initial guesses for $f''(0)$ and $\theta'(0)$ are not explicitly provided in the text but are typically chosen based on physical insight, prior studies (e.g., Uka et al. [45]), or simplified analytical solutions. For example, if the problem involves boundary layer flow or heat transfer, guesses may be derived from similar problems or asymptotic analysis.

- Strategy: A common approach is to start with small, physically reasonable values $(e.g., f''(0) = 0.1, \theta'(0) = 0.1)$ or values from a related linear problem. Multiple guesses may be tested to ensure the shooting method converges to the correct solution.
- Impact: Poor initial guesses can lead to divergence or convergence to incorrect solutions, so they are often refined iteratively based on the shooting algorithm's feedback.

3. Tolerances:

- Definition: Tolerances refer to the acceptable error in satisfying the boundary conditions $f(\infty) = 0 \; and \; \theta(\infty) = 0 \; at \; \eta = \eta_\infty$, as well as the accuracy of the computed slopes $f''(0)$ and $\theta'(0)$.
- Typical Values: While not specified in the text, standard tolerances for such numerical methods are on the order of 10^{-4} to 10^{-6} for boundary condition residuals $(e.g., |f(\eta_\infty)| < 10^{-6}, |\theta(\eta_\infty)| < 10^{-6})$. For the Runge–Kutta–Fehlberg method, the local truncation error is controlled to a similar precision $(e.g., 10^{-6})$.
- Implementation: The Runge–Kuttab–Fehlberg method uses an adaptive step size to maintain the specified tolerance, adjusting the step size to minimize error while optimizing computational efficiency. Newton's method, used for iterating the slopes, typically requires a tolerance for the change in $f''(0) \; and \; \theta'(0)$ between iterations $(e.g., |\Delta f''(0)| < 10^{-6})$.
- Trade-offs: Tighter tolerances improve accuracy but increase computational time. The choice depends on the desired precision and available computational resources.

4. Convergence Checks:

- Shooting Method Convergence: The shooting method iteratively adjusts $f''(0)$ and $\theta'(0)$ using Newton's method to minimize the error in the boundary conditions at $\eta = \eta_\infty$. Convergence is achieved when $|f(\eta_\infty)|$ and $|\theta(\eta_\infty)|$ are within the specified tolerance $(e.g., 10^{-6})$.
- Newton's Method: For each iteration, Newton's method solves for updates to $f''(0)$ and $\theta'(0)$ by linearizing the system around the current guess. Convergence is confirmed when the updates become sufficiently small $(e.g., |\Delta f''(0)| < 10^{-6}, |\Delta\theta'(0)| < 10^{-6})$ and the boundary conditions are satisfied.
- Runge–Kuttab–Fehlberg Method: This method ensures convergence of the ODE solution by controlling the local truncation error through its embedded error estimation (comparing fourth- and fifth-order approximations). The adaptive step size ensures that the solution remains stable and accurate across the domain $[0, \eta_\infty]$.

  Additional Checks: Convergence is further validated by comparing the computed values of $f(\eta)$ and $\theta(\eta)$ with the benchmark solution from Uka et al. [45]. An agreement within a small error $(e.g., relative\ error < 1\%)$ confirms the reliability of the numerical solution. Sensitivity analysis, such as varying $\eta\infty$ or initial guesses, may also be performed to ensure robustness.

3. Results and Discussions

This study involves a steady state Maxwell fluid, focusing on melting heat and null mass flux at the flow boundary.

As earlier described in the body of literature, Maxwell fluid exhibit both viscous and elastic responses and this is crucial in many applications both in engineering and in the biological field.

The mathematical equations were an enhancement of the well-known Navier Stokes equations, coupled and nonlinear in the context of this study.

The nonlinear equations were converted to a non-linear coupled *ODEs*, which were treated with MAPLE software.

The detail results are discussed below.

The consistency of this present effort with existing literature is conveyed in Table 1, and this has further highlighted the alignment of the present paper with existing scientific output in the field of fluid dynamics. Fig. 2 presents magnetic field's influence on velocity.

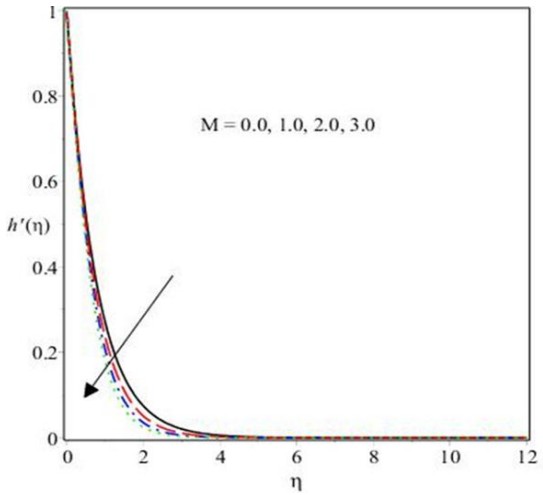

Figure 2. Effect of *M* on Velocity

The profile depicts a decrease in velocity with increasing magnetic field. The fluids that are electrically activated contains charged particle, these charged particles experience a force (Loretz force) when Magnetic field is applied, causing the charges to move in the field's direction. This force influences the direction of the magnetic field and provide a background for the fluid's current. Lorentz force has the tendency to either inhibit or promote the fluid's flow.

Moreover, the fluid may experience magnetic tension from the magnetic field, which tends to limit or soften the flow.

The overall result is a drop in the velocity profile of the fluid, particularly in regions with a strong magnetic field. Generally speaking, turbulence improves fluid velocity and mixing. The velocity profile decreases as turbulence is suppressed, creating a more orderly and less dynamic flow.

Table 1. Comparison for Prandtl number for $k = R = Sc = 1.0$ and $\beta = 0.1$

P_r	[11]	[20]	[2]	Present Result
0.72	0.46315	0.46310	0.46315	0.35612
1.00	0.58199	0.58200	0.58200	0.51432
3.00	1.16523	1.16520	1.16530	1.17122
10.0	2.30796	2.30800	2.30835	2.40124

Fig. 3 and Fig. 4 illustrate the radiative impact on the profiles of h' and θ. The fluid's velocity increases inversely with the radiative parameter.

The chart clearly indicates that velocity diminishes as the radiation parameter increases across different values. Additionally, as Fig. 4 illustrates, a decrease in the conduction effect and thermal boundary layer occurs with an increase in R.

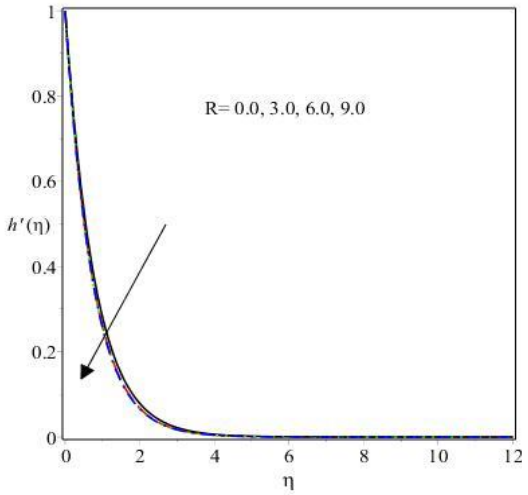

Figure 3. Effect of R on Velocity

The consequence of melting heat stimulus on the velocity is shown in Fig. 5. Evidently, a higher melting heat parameter leads to a higher velocity profile as depicted in the graph.

This behavior is akin to fluid dynamics involving in phase transition processes, and the latent heat of melting. Recall that heat energy is absorbed by a substance as it transits from one phase to another, thereby increasing the temperature in the process.

The process of changing from a solid to a liquid is called" latent melting."

The latent melting heat is the amount of heat needed to crush the intermolecular forces that binds solids. The system enables this phase transition by transferring heat energy, as evidenced by an enhancement in the melting heat effect. The solid melts into liquid at a faster rate as a result of the additional energy.

Moreover, increasing the system's temperature can cause the fluid to move and conform more vigorously. An elevated velocity profile is the result of the increased energy encouraging higher fluid velocities.

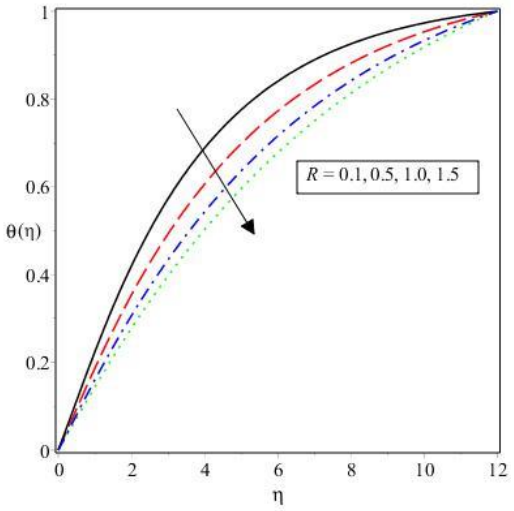

Figure 4. Effect of R on Temperature

However, there is a contrasting development in Fig. 6, where the temperature decreases as the melting heat parameter increases.

This observation implies that a small melting heat value is caused by the free stream temperature T_∞ being equal to the surface temperature T_m approximately.

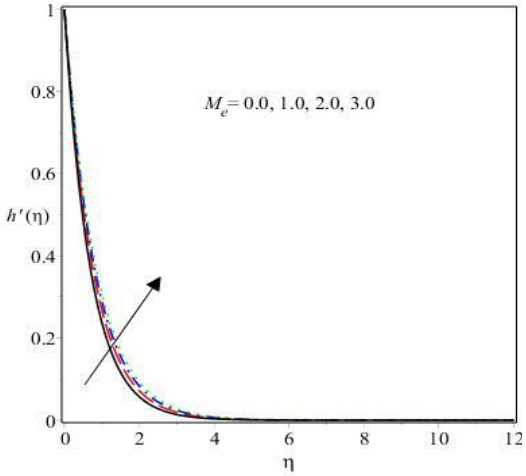

Figure 5. Effect of Me on Velocity

Fig. 7 portrays the effect of β on the velocity. It denotes the temporal reaction of a viscoelastic fluid to applied forces.

β is a parameter commonly used in medicine to evaluate the rate at which a viscoelastic material reacts to an applied stress.

Additionally, a high β portrays that the material exhibits rapid feedback to deformation and may readily return to its initial shape. This rapid reaction to deformation enhances force transmission, resulting in increased velocities as β rises. This stands in sharp contrast to low β, when the material exhibits a more pronounced viscous reaction and is unable to promptly recover its original shape following deformation.

Consequently, with low β, the velocity diminishes due to the inertial viscous properties that impede the material's ability to restore its original shape.

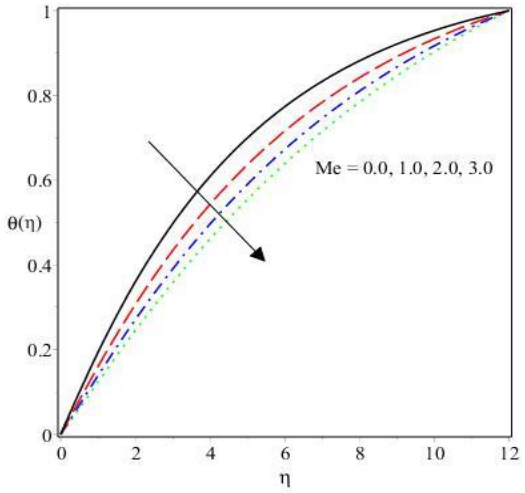

Figure 6. Effect of *Me* on Temperature

It is important to note that the specific behavior is determined by the material qualities and the characteristics of the fluid in question. In viscoelastic systems, an increase in β typically elicits a greater elastic response, which consequently leads to an enhanced velocity profile as the material adjusts to changes in flow dynamics.

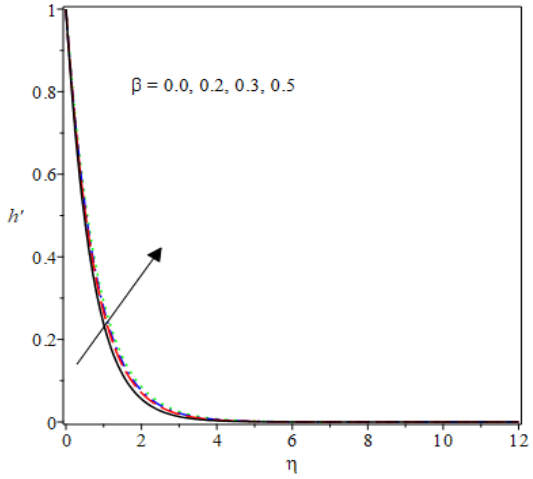

Figure 7. Effect of $\boldsymbol{\beta}$ on Velocity

The effect of P_r on temperature distribution is seen in Fig. 8 . The figure portrays a rise in temperature due to the interplay between heat transfer kinematics and the comparative rates of momentum and thermal diffusion.

The fluid's effectiveness to transfer momentum, in comparison to heat transfer, is indicated by a higher Prandtl number.

This shows that thermal diffusion within the fluid takes a different rate than momentum diffusion. Therefore, the fluid shows an increased ability to mix and transfer heat effectively as the P_r increases. This enhanced thermal diffusion suggests that thermal energy is transferred through the fluid more efficiently, which raises the fluid's temperature. Fig. 9 illustrates the impact of porosity on velocity.

The velocity diminishes as the porosity increases, indicating that a heightened porosity diminishes fluid's velocity within the medium. Increased porosity elevates flow resistance, distorting the streamline pattern and diminishing overall velocity. This effect is essential for understanding fluid dynamics in porous media, particularly in applications related to filtration, oil recovery, and groundwater flow.

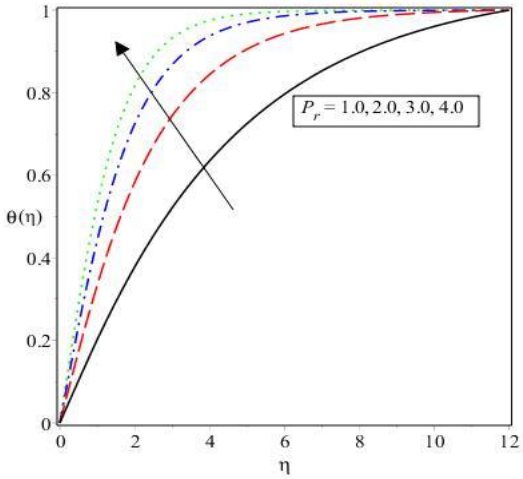

Figure 8. Effect of ***Pr*** on Temperature

The physical implication indicates that as porosity grows, the medium becomes increasingly porous. This generates additional empty spaces inside the medium, so augmenting the surface area in contact with the fluid. The augmented surface area generates greater frictional resistance for the fluid's flow, thereby diminishing the total velocity.

Furthermore, concerning the diminished effective area, it is a widely recognized principle that in a porous media, fluid traverses the interlinked pores.

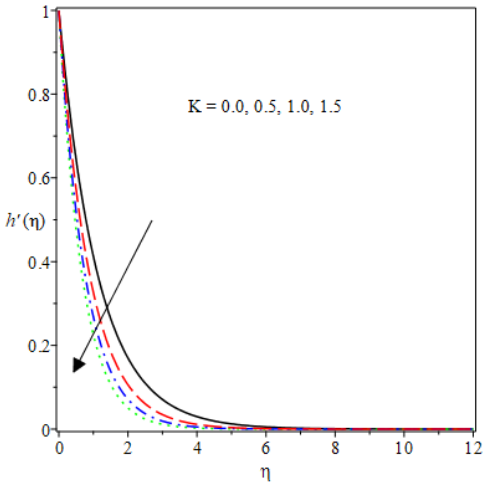

Figure 9. Effect of ***K*** on velocity

As porosity increases, resulting in additional void spaces, the fluid traverses a longer and more convoluted path, hence diminishing the flow velocity across the medium. In the context of energy dissipation within a porous medium, fluid particles undergo swift collisions with the solid matrix. This recurrent impact decreases the fluid's kinetic energy, resulting in a decrease in velocity. This decline becomes more evident with heightened porosity.

4. Conclusions

In this study we have considered melting heat transfer effect, MHD, radiation, and channel porosity in our analysis. The MAPLE software was used to scrutinize the equations numerically and present the key profiles. The key results below are worth mentioning;

The fluid experience increases in velocity profile and this is occasioned by a steady rise in the magnetic field parameter. A steady increase in the melting heat transfer parameter enhances the velocity profile, thereby increasing the velocity of the fluid.

A rise in the Prandtl number corresponds to an increase in temperature distribution throughout the fluid. Furthermore, it illustrates the fluid's ability to transfer momentum more effectively than heat. An increase in the Deborah number promotes an increase in the fluid's velocity. Fluid velocity and temperature profiles experiences a decline as the radiation parameter increases steadily

Fluid velocity and temperature profiles diminish as the radiation parameter increases steadily. The observed variations in temperature profiles demonstrate the complex interaction between fluid dynamics and heat transfer processes. This interaction highlights the necessity of integrating MHD and other parameters to comprehend and manage temperature distributions in pertinent systems. The paper emphasizes the essential application of magnetohydrodynamics (MHD), thermal radiation, and melting heat in optimizing thermal management strategies, thereby improving the efficiency of diverse engineering systems, such as plasma devices, liquid metals, cooling systems, and magnetically driven flows.

5. Future Possibilities

Through the reviews and the computational analysis in this present study, our aim is to provide room for other scholars' valuable resources to further the studies on viscoelastic fluids. Following the outcomes from this study future studies could explore the effects of varying operational conditions such as types of geometries, and other fluid types, such as third grade, Sisko, and micropolar fluids with the implementation of the same or different parameters. Furthermore, such work should consider different geometries and coordinate systems.

The proposed concepts will create opportunities for more results-oriented applications, thereby expanding the scope of research.

Authors Contribution
All authors conceived of the study, participated in its design and coordination, drafted the manuscript, participated in the sequence alignment, and read and approved the final manuscript.

Availability of data and materials
Not applicable. In fact, all results are obtained without any software and found by manual computations. In other words, the manuscript is in the pure mathematics (mathematical analysis) category.

Conflict of interests
The author states that there is no conflict of interest.

References

[1] K. Sudarmozhi, D. Iranian, S. Alqahtani, I. Khan, and S. Niazai, "Viscoelasticity of Maxwell fluid in a permeable porous channel," Discov. Mech. Eng., vol. 3, no. 1, p. 27, Sep. 2024, doi: 10.1007/s44245-024-00061-8

[2] R. G. Abdel-Rahman, M. M. Khader, and A. M. Megahed, "Melting phenomenon in magneto hydro-dynamics steady flow and heat transfer over a moving surface in the presence of thermal radiation," Chinese Phys. B, vol. 22, no. 3, p. 030202, Mar. 2013, doi: 10.1088/1674-1056/22/3/030202

[3] H. Hanif, "A computational approach for boundary layer flow and heat transfer of fractional Maxwell fluid," Math. Comput. Simul., vol. 191, pp. 1–13, Jan. 2022, doi: 10.1016/j.matcom.2021.07.024

[4] E. A. Algehyne, F. M. Alamrani, S. Shahab, Z. Khan, S. A. Lone, and A. Saeed, "Significance of Rosseland's radiative heat transfer and dissipative heat on MHD viscous flow over a slandering sheet in the presence of Darcy-Forchheimer and Lorentz forces," Proc. Inst. Mech. Eng. Part E J. Process Mech. Eng., vol. 0, no. 0, Apr. 2024, doi: 10.1177/09544089241242956

[5] M. L. De Haro, J. A. P. Del Río, and S. Whitaker, "Flow of Maxwell fluids in porous media," Transp. Porous Media, vol. 25, no. 2, pp. 167–192, Nov. 1996, doi: 10.1007/BF00135854

[6] S. Karra, V. Průša, and K. R. Rajagopal, "On Maxwell fluids with relaxation time and viscosity depending on the pressure," Int. J. Non. Linear. Mech., vol. 46, no. 6, pp. 819–827, Jul. 2011, doi: 10.1016/j.ijnonlinmec.2011.02.013

[7] K. Sudarmozhi, D. Iranian, and I. Khan, "A steady flow of MHD Maxwell viscoelastic fluid on a flat porous plate with the outcome of radiation and heat generation," Front. Phys., vol. 11, Jun. 2023, doi: 10.3389/fphy.2023.1126662

[8] T. Hayat, M. Hussain, M. Awais, and S. Obaidat, "Melting heat transfer in a boundary layer flow of a second grade fluid under Soret and Dufour effects," Int. J. Numer. Methods Heat Fluid Flow, vol. 23, no. 7, pp. 1155–1168, Sep. 2013, doi: 10.1108/HFF-09-2011-0182

[9] S. A. Agunbiade, t. L. Oyekunle, and m. T. Akolade, "Radiative and mhd dissipative heat effects on upper-convected maxwell fluid flow and material time relaxation over a permeable stretched sheet," comput. Therm. Sci. An int. J., vol. 15, no. 3, pp. 45–59, 2023, doi: 10.1615/computthermalscien.2022043596

[10] M. S. Abel, J. V. Tawade, and J. N. Shinde, "The Effects of MHD Flow and Heat Transfer for the UCM Fluid over a Stretching Surface in Presence

of Thermal Radiation," Adv. Math. Phys., vol. 2012, pp. 1–21, 2012, doi: 10.1155/2012/702681

[11] N. A. Yacob, A. Ishak, and I. Pop, "Melting heat transfer in boundary layer stagnation-point flow towards a stretching/shrinking sheet in a micropolar fluid," Comput. Fluids, vol. 47, no. 1, pp. 16–21, Aug. 2011, doi: 10.1016/j.compfluid.2011.01.040

[12] R. Agrawal, S. K. Saini, and P. Kaswan, "Numerical modeling of MHD micropolar fluid flow and melting heat transfer under thermal radiation and Joule heating," Int. J. Comput. Methods Eng. Sci. Mech., vol. 24, no. 2, pp. 143–154, Mar. 2023, doi: 10.1080/15502287.2022.2113183

[13] J. Cui, F. Azam, U. Farooq, and M. Hussain, "Non-similar thermal transport analysis in entropy optimized magnetic nanofluids flow by considering effective Prandtl number model with melting heat transfer and Joule heating," J. Magn. Magn. Mater., vol. 567, p. 170331, Feb. 2023, doi: 10.1016/j.jmmm.2022.170331

[14] L. Ebiwareme, E. Esekhaigbe, K. W. Bunonyo, and U. A. Uka, "Magnetohydrodynamic Nonlinear Radiative Heat and Mass Transfer Flow of Sisko Nanofluid through a Nonlinear Stretching Sheet in The Presence of Chemical Reaction," J. Adv. Math. Comput. Sci., vol. 38, no. 11, pp. 72–86, Dec. 2023, doi: 10.9734/jamcs/2023/v38i111846

[15] E. Esekhaigbe, U.A. Uka and A. Musa., "Magnetohydrodynamic Effects on the Flow of Nanofluids Across a Convectively Heated Inclined Plate Through a Porous Medium with a Convective Boundary Layer," Int. J. Mater. Math. Sci., pp. 41–51, Oct. 2023, doi: 10.34104/ijmms.023.041051

[16] B. Sun, W. Lei, and D. Yang, "Flow and convective heat transfer characteristics of Fe2O3–water nanofluids inside copper tubes," Int. Commun. Heat Mass Transf., vol. 64, pp. 21–28, May 2015, doi: 10.1016/j.icheatmasstransfer.2015.01.008

[17] M. Khan, R. Malik, A. Munir, and W. A. Khan, "Flow and Heat Transfer to Sisko Nanofluid over a Nonlinear Stretching Sheet," PLoS One, vol. 10, no. 5, p. e0125683, May 2015, doi: 10.1371/journal.pone.0125683

[18] K. Gangadhar, M. Venkata Subba Rao, and P. R. Sobhana Babu, "Numerical analysis for steady boundary layer flow of Maxwell fluid over a stretching surface embedded in a porous medium with viscous dissipation using the spectral relaxation method," Int. J. Ambient Energy, vol. 42, no. 13, pp. 1492–1498, Oct. 2021, doi: 10.1080/01430750.2019.1611641

[19] M. Jawad, M. Alam, M. K. Hameed, and A. Akgül, "Numerical simulation of Buongiorno's model on Maxwell nanofluid with heat and mass transfer using Arrhenius energy: a thermal engineering implementation," J. Therm. Anal. Calorim., vol. 149, no. 11, pp. 5809–5822, Jun. 2024, doi: 10.1007/s10973-024-13133-4

[20] X.-H. Zhang, R. Shah, S. Saleem, N. A. Shah, Z. A. Khan, and J. D. Chung, "Natural convection flow maxwell fluids with generalized thermal transport and newtonian heating," Case Stud. Therm. Eng., vol. 27, p. 101226, Oct. 2021, doi: 10.1016/j.csite.2021.101226

[21] A. Ishak, "Thermal boundary layer flow over a stretching sheet in a micropolar fluid with radiation effect," Meccanica, vol. 45, no. 3, pp. 367–373, Jun. 2010, doi: 10.1007/s11012-009-9257-4

[22] A. Raza et al., "Natural convection flow of radiative maxwell fluid with Newtonian heating and slip effects: Fractional derivatives simulations," Case Stud. Therm. Eng., vol. 28, p. 101501, Dec. 2021, doi: 10.1016/j.csite.2021.101501

[23] A. U. Rehman, M. B. Riaz, A. Atangana, F. Jarad, and J. Awrejcewicz, "Thermal and concentration diffusion impacts on MHD Maxwell fluid: A generalized Fourier's and Fick's perspective," Case Stud. Therm. Eng., vol. 35, p. 102103, Jul. 2022, doi: 10.1016/j.csite.2022.102103

[24] K. Gangadhar, M. Prameela, A. J. Chamkha, B. G R, and T. Kannan, "Evaluation of homogeneous-heterogeneous chemical response on Maxwell-fluid flow through spiraling disks with nonlinear thermal radiation using numerical and regularized machine learning methods," Int. J. Model. Simul., pp. 1–23, Mar. 2024, doi: 10.1080/02286203.2024.2327598

[25] M. Rupa Lavanya, K. Gangadhar, D. N. Bhargavi, and A. J. Chamkha, "Chemical response in Oldroyd-B liquid through rotational disk with temperature and space-related heat rise," Mod. Phys. Lett. B, vol. 39, no. 28, Oct. 2025, doi: 10.1142/S0217984925501465

[26] N. Gomathi and D. Poulomi, "Entropy optimization on EMHD Casson Williamson penta-hybrid nanofluid over porous exponentially vertical cone," Alexandria Eng. J., vol. 108, pp. 590–610, Dec. 2024, doi: 10.1016/j.aej.2024.07.092

[27] M. Khan, D. Lu, G. Rasool, W. Deebani, and S. M. Shaaban, "Fractional numerical analysis of γ-Al2O3 nanofluid flows with effective Prandtl number for enhanced heat transfer," J. Comput. Des. Eng., vol. 11, no. 4, pp. 319–331, Jul. 2024, doi: 10.1093/jcde/qwae071

[28] N. Gomathi and. De. Poulomi, "Bioconvectional non-newtonian nanofluid flow due to swimming microorganisms with hall current and ion slip over porous medium: a statistical analysis approach," spec. Top. Rev. Porous media an int. J., vol. 16, no. 1, pp. 63–81, 2025, doi: 10.1615/SpecialTopicsRevPorousMedia.2024052306

[29] K. Gangadhar, G. Naga Chandrika, and S. Dinarvand, “Thermal memory effect and Joule heating on squeezed flow through a Riga surface with a Darcy porous medium,” Int. J. Ambient Energy, vol. 45, no. 1, Dec. 2024, doi: 10.1080/01430750.2024.2439425

[30] S. Sireesha, K. Gangadhar, and S. Dinarvand, “Comparative energy performance in Au/H2O, Au–Ag/H2O and Au–Ag–MWCNT/H2O with shape factor with heat generation impact,” Mod. Phys. Lett. B, vol. 39, no. 31, Nov. 2025, doi: 10.1142/S0217984925501830

[31] K. Gangadhar, E. Mary Victoria, and A. Wakif, “Irreversibility analysis for the EMHD flow of silver and magnesium oxide hybrid nanofluid due to nonlinear thermal radiation,” Mod. Phys. Lett. B, vol. 38, no. 33, Nov. 2024, doi: 10.1142/S0217984924503378

[32] K. Gangadhar, N. C. G, and S. Dinarvand, “Stagnation point of the triple nanoparticle nanofluid flow through the spinning sphere with radiation absorption,” Pramana, vol. 98, no. 3, p. 95, Jul. 2024, doi: 10.1007/s12043-024-02768-5

[33] K. Gangadhar, T. Sujana Sree, and A. J. Chamkha, “Binary chemical interaction and nonlinearity radiative flux of Williamson fluidic flow through Riga plate,” Int. J. Model. Simul., pp. 1–15, Feb. 2024, doi: 10.1080/02286203.2024.2318753

[34] N. Gomathi and De. Poulomi, “Three-dimensional rotating, unsteady casson williamson nanofluid flow with activation energy and chemical reaction over darcy-forchheimer porous media,” j. Porous media, vol. 28, no. 8, pp. 45–71, 2025, doi: 10.1615/jpormedia.2024052174

[35] M. Khan, M. Imran, M. R. Khan, S. A. O. Beinane, and A. Alzahrani, “Numerical Analysis of Heat Transfer and Flow Characteristics of Jeffrey Nanofluid Over Stretched Surfaces With MHD and Slip Effects,” Math. Methods Appl. Sci., vol. 48, no. 8, pp. 8641–8653, May 2025, doi: 10.1002/mma.10742

[36] M. Khan, A. Rasheed, M. S. Anwar, and S. T. Hussain Shah, “Application of fractional derivatives in a Darcy medium natural convection flow of MHD nanofluid,” Ain Shams Eng. J., vol. 14, no. 9, p. 102093, Sep. 2023, doi: 10.1016/j.asej.2022.102093

[37] M. S. Anwar, T. Muhammad, M. Khan, and V. Puneeth, “MHD nanofluid flow through Darcy medium with thermal radiation and heat source,” Int. J. Mod. Phys. B, vol. 38, no. 28, Nov. 2024, doi: 10.1142/S0217979224503867

[38] M. Khan and M. Imran, “ANN-driven insights into heat and mass transfer dynamics in chemical reactive fluids across variable-thickness surfaces,” Heat Transf., vol. 53, no. 8, pp. 4551–4571, Dec. 2024, doi: 10.1002/htj.23144

[39] M. Khan and A. Rasheed, “Slip velocity and temperature jump effects on molybdenum disulfide MoS2 and silicon oxide SiO2 hybrid nanofluid near irregular 3D surface,” Alexandria Eng. J., vol. 60, no. 1, pp. 1689–1701, Feb. 2021, doi: 10.1016/j.aej.2020.11.019

[40] [40]M. Khan, S. A. Lone, A. Rasheed, and M. N. Alam, “Computational simulation of Scott-Blair model to fractional hybrid nanofluid with Darcy medium,” Int. Commun. Heat Mass Transf., vol. 130, p. 105784, Jan. 2022, doi: 10.1016/j.icheatmasstransfer.2021.105784

[41] M. S. Anwar, M. Khan, Z. Hussain, T. Muhammad, and V. Puneeth, “Investigation of heat transfer characteristics in MHD hybrid nanofluids with variable viscosity and thermal radiations,” J. Radiat. Res. Appl. Sci., vol. 18, no. 1, p. 101240, Mar. 2025, doi: 10.1016/j.jrras.2024.101240

[42] K. Aghayeva and G. Krauklit, “Radiative transfer model application with satellite imagery for methane emission analysis,” J. Theor. Appl. Phys., vol. 19, no. 4, 2025, doi: 10.57647/j.jtap.2025.1904.36

[43] A. Ramar et al., “Melting heat effect in MHD flow of maxwell fluid with zero mass flux,” Case Stud. Therm. Eng., vol. 53, p. 103910, Jan. 2024, doi: 10.1016/j.csite.2023.103910

[44] K. Kumar Ch. and S. Bandari, “Melting heat transfer in boundary layer stagnation-point flow of a nanofluid towards a stretching–shrinking sheet,” Can. J. Phys., vol. 92, no. 12, pp. 1703–1708, Dec. 2014, doi: 10.1139/cjp-2013-0508

[45] U. Uka, E. Esekhaigbe, D. Idıka, G. Kalu, and K. Agbo, “Thermal Performance Analysis of Tilted Fin Arrays with Temperature-Dependent Viscous Dissipation and Material Effects in Heat Exchange Systems,” Amesia, vol. 6, no. 1, pp. 57–81, Jun. 2025, doi: 10.54559/amesia.1730032